FINEST FILAMENTARY STRUCTURES OF THE CORONA IN THE SLOW AND FAST SOLAR WIND

Richard Woo
Jet Propulsion laboratory, California Institute of Technology, 4800 Oak Grove Drive, MS 238-725, Pasadena, CA 91109

Shadia R. Habbal
Harvard-Smithsonian Center for Astrophysics, 60 Garden Street
Cambridge, MA 02138

Recent progress in our understanding of electron density fluctuations observed by radio occultation measurements has demonstrated that a break in the vicinity of 1 Hz in the temporal frequency spectrum of the density fluctuations provides a measure of the size of the finest filamentary structures in the solar corona. Break frequencies have been inferred from the density spectra deduced from 1979-1980 Voyager phase scintillation and spectral broadening measurements by Colts et al. [1991]. These results show that the finest filamentary structures are found in the extensions or stalks of coronal streamers where the density fluctuations are enhanced - the likely sources of the slow solar wind — and are over a factor of three smaller than those in the fast wind emanating from coronal holes. The inferred sizes of the finest filamentary structures are approximately 6 km in the slow wind at 8 $R_\odot$ and 22 km in the fast wind at 9.1 $R_\odot$.

Subject headings: interplanetary medium — solar wind --- Sun: corona

Submitted April 4, 1996 to Astrophysical Journal Letters

Revised September 25, 1996

1. INTRODUCTION

Coronal streamers and polar plumes are prominent raylike structures that have long been observed in solar eclipse and white-light coronagraph measurements. There is growing evidence that the corona is permeated by a hierarchy of raylike structures extending from these large-scale structures all the way down to kilometer size structures at the Sun [Koutchmy 1988; Karovska and Habbal 1991; Woo et al. 1995; November and Koutchmy 1996; Woo 1996]. Evidence for the finest structures or flux tubes that rotate with the Sun comes from angular broadening measurements, which offer probing capabilities that surpass those of conventional imaging techniques in the visible, radio, extreme ultraviolet, and x-rays [Woo 1996].

The purpose of this letter is to show that the sizes of finest filamentary structures depend on the source regions of the solar wind. The basis for these studies is summarized in the following section before the finest structures are inferred from radio occultation measurements in section 3, and the conclusions are given in section 4.

2. BACKGROUND

Angular broadening measurements have been conducted since the 1950s [Hewish, 1958; Vitkevitch, 1959; Erickson, 1964]. These interferometric measurements yield information on density variations in the plane of the sky having spatial scales comparable to the interferometer baselines, 1-35 km at the VLA [Armstrong et al. 1990] and 0.2-2 km at Culgoora [Ward 1975]. Observation of radially expanding flux tubes by the VLA and Culgoora is illustrated schematically in Fig. 1. The circles depicting the longest baselines, and hence the largest scales probed by each observatory, lie within the flux tubes at 10 $R_\odot$. Since the small-scale turbulence that is convected with the solar wind inside the flux tubes is nearly isotropic, scattering transverse to the flux tubes (magnetic field) is about roughly

the same as that parallel to flux tubes, and the observed angular broadening is approximately isotropic.

Closer to the Sun, when the longest transverse baseline exceeds the size of the flux tube, scattering is stronger transverse to the flux tube than along it, so that the observed angular broadening is anisotropic [SCC Fig. 1 of Narayan et al., 1989 for example of an angular broadened anisotropic image; Armstrong et al., 1990; Anantharamaiah et al., 1994]. The structure function characterizes the distribution of fluctuation power with scale sizes. Anisotropy occurs because the structure function of scales transverse to the flux tube and larger than the flux tube is steeper than that of corresponding scales along the flux tube (the structure function will be described in more detail later). Since the longer transverse baselines intercept the flux tubes first, the observed aniostropy is higher at the VLA than at Culgoora in the range of 5-10 $R_\odot$ [Armstrong et al. 1990].

in terms of in situ plasma measurements, angular broadening is analogous to having multiple spacecraft dispersed in the plane of the sky, measuring the density variations between them, and characterizing them in terms of their structure function or spatial spectrum; these arc spatial measurements. The structure function CLOSC to the Sun, where high anisotropy of angular broadening is observed, is schematically summarized in Fig. 2. Inside the flux tubes (s smaller than the transverse dimension of the flux tube D), the small-scale turbulence is nearly isotropic, and the structure functions in the parallel and transverse directions arc essential] y the same; it varies approximatel y as s^1. For scales exceeding D, the structure function in the transverse direction steepens to $s^{5/3}$ (Kolmogorov case), while that along the flux tubes continues ass].

Other than observing path-integrated density instead of density at a point, the measurement of phase scintillation is similar to the in situ measurement of plasma density by a spacecraft, Variations in solar wind density arc observed: (1) as turbulent plasma that is convected along the solar wind within the flux tubes flows past the spacecraft, and (2) as flux tubes move across the spacecraft. The temporal variation of density is characterized by

the frequency spectrum of the density fluctuations, which shows a break near 1 Hz separating the. turbulence regime at the higher frequencies from the flux tube regime at the lower frequencies. in the case of convected turbulence., the frequency spectrum is related to the structure function in the direction of the, solar wind flow (roughly parallel to the magnetic field) through the solar **wind** speed. On the other hand, in the absence of temporal variations at the Sun, the spectrum of density fluctuations across the flux tubes is related to the structure function transverse to the magnetic field through the relative motion of the spacecraft transverse to the flux tubes, For a spacecraft located off the limb of the Sun at low latitude, this is the rotation rate of the Sun. Finally, spectral broadening observes the high frequency portion of the frequency spectrum of density fluctuations (turbulence), which is related to the structure function in the flow direction of the solar wind.

From the preceding discussion, it is clear that the onset of high anisotropy in angular broadening is onc measure of tbc flux tube size in the corona, and the break in the frequency spectrum of the density fluctuations deduced from phase scintillation and spectral broadening measurements is another. Estimates of the flux tube sizes obtained from these independent but complementary methods yield kilometer scale sizes that arc mutually consistent [Woo 1996].

Although studies of the density spectrum have been based on a variety of radio occultation measurements [Cronyn 1970, Hewish 1971, Cronyn 1972, Jokipii 1973, Lotova 1975, Colts 1978], the availability of phase scintillation and spectral broadening measurements of spacecraft radio signals has made it possible to observe the spectrum over a wide range of fluctuation frequencies [Callahan 1975, Woo et al. 1976a,b, Woo and Armstrong 1979, Martin 198S] and establish the break near 11 Hz [Colts et al. 1991]. In situ measurements beyond 0.3 AU have shown major differences between the density spectrum of the slow-speed wind associated with the streamer belt and that of the fast solar wind emanating from coronal holes [Marsch and Tu 1990]. However, separate characterizations of these two types of wind in their source regions near the Sun have not

been made with radio occultation measurements, because of the lack of simultaneous velocity measurements. Recent progress has shown that knowledge of the morphology of density fluctuations in the corona [Woo and Gazis 1993; Woo et al. 1995] and solar wind [Huddleston et al. 1995] can be used to distinguish the slow and fast solar wind. Low levels of density fluctuations and scintillation are associated with the fast wind from coronal holes, while prominent enhancements are the signature of the extensions or stalks of coronal streamers, the like] y sources of the slow solar wind [Woo 1995] observed beyond 0.3 AU by in situ plasma measurements near the heliospheric current sheet [Gosling et al. 198 1; Marsch and Tu 1990; Winter-halter et al. 1994; Huddleston et al. 1995].

in the following section, wc will usc the breaks in the density spectra observed in 1979-1980 Voyager phase scintillation and spectral broadening measurements [Coles et al. 1991] to infer the finest filamentary structures, and the morphology of the corona to identify the source regions of the fast and slow solar wind.

3. VOYAGER MEASUREMENTS 01 THE DENSITY SPECTRUM

Radio occultation measurements conducted during the conjunctions of Voyager 1 and Voyager 2 in 1979-1982 have been dc.scribed by Martin [1985]. Reproduced in Fig. 3 from Fig. 3a of Colts et al. [1991] arc the structure functions deduced from the Voyager phase scintillation and spectral broadening measurements, covering a heliocentric distance range of 7.1-9.8 R_o. Error analyses of these structure functions have been discussed by Colts et al. [1991] in their appendix B. The structure functions in Fig. 3 were not obtained from spatial measurements, but were instead deduced from temporal variations assuming turbulence convected along the solar wind. Since we arc interested in the temporal frequency spectrum of the density fluctuations, and since this is what was original] y measured by Colts et al [1991], wc have converted the spatial scales back to the originally observed fluctuation frequencies. To preserve the original figure of Colts et al.

[1991], the corresponding frequency scale has simply been added to the abscissa, and we " will refer to the results in Fig. 3 as density spectra,

The uppermost spectrum in Fig. 3 was observed by Voyager 2 on August 17, 1979 (DOY 229) at a closest approach distance of 8 R_O, while the lowermost on September 20, 1980 (DOY 264) at a closest approach distance of 9.1 R_O. Shown in Fig. 4 arc the contour maps of the source surface magnetic field strength produced by the Wilcox Solar Observatory for Barrington Rotations (CR)1684 and 1699, respectively [1 locksema and Scherrer 1986]. The closest approach points of the Voyager 2 radio paths have been mapped back to the Sun assuming a solar wind speed of 450 km/s and represented by dots on the contour maps. The mapping results arc not sensitive to the assumed solar wind speed because the measurements took place close to the Sun, The CR 1684 map shows that on August 17, 1979 Voyager 2 probed a region near an evolving neutral line region (SCC also source surface field map of CR 1685 in Hocksema and Scherrer [1986]), where slow wind would be expected. In contrast, the CR 1699 map in Fig. 4 shows that on September 20, 1980 Voyager 2 probed a corona] hole, the source of the fast solar wind.

Estimates of solar wind velocity were obtained by Martin [1985] from an analysis of the power spectrum of the intensity scintillations. The uncertainty in these velocities near the Sun can be high, owing to the anisotropy of the density irregularities, the presence of random velocities, and the interdependence between axial ratio, random and mean velocity, as discussed by Martin [1985]. Still, the velocity estimates of 320 ±80 km/s on August 17, 1979 and 483 ±100 km/s on September 20, 1980 measurements, are consistent with the uppermost and lowermost spectra in Fig. 3 pertaining to the contrasting slow and fast solar wind, respectively. Like the slow wind spectrum near 0.3 AU from in situ measurements [Marsch and Tu 1990], the slow wind spectrum in Fig. 3 is an order of magnitude higher than that of the fast wind.

The uppermost spectrum represents one of four 'transients' in the Colts et al. study [1990], Doppler/phase scintillation transients have mainly represented propagating

disturbances whose speeds were higher than those of the ambient solar wind [Woo and Armstrong 1981, Woo et al, 1985, Woo ant] Schwenn 1991]. in fact, another one of the four 'transients' identified in the Colts et al. [1991] study -- that of August 26, 1979 (DOY 238) by Voyager 1 --- was also located near the heliospheric current sheet, but appears to have been a propagating disturbance since its velocity of 820 km/s was the highest in the extensive 1979-1982 Voyager data set estimated by Martin [1985], The slow velocity of the uppermost spectrum in Fig. 3 is unusual for a transient, and provides corroborating evidence that it represents a coronal streamer [Woo et al. 1995] rather than a propagating interplanetary disturbance associated with a coronal mass ejection [Woo 1993].

The breaks in the uppermost and lowermost power-law density spectra in Fig. 3 have been determined through a best fit of a two-line model by eye, and occur near fluctuation frequencies of 2.6 and 0.76 Hz, respectively. Assuming that the finest structures rotate with the Sun, these frequencies translate to approximate transverse sizes of 6 km in the slow wind at $8\,R_O$ and 22 km in the fast wind at 9.1 R_O, the latter being consistent with the fast wind results in Woo [1996], The finest filamentary structures are hence more than a factor of three finer in the slow than the fast wind. Extrapolating the finest filamentary structures back to the Sun assuming radial expansion of the flux tubes yields approximate transverse sizes at the Sun of 0.7 and 2.4 km for the slow and fast wind, respectively.

4. DISCUSSION AND SUMMARY

Motivated by the ubiquity of raylike structures in the solar corona, extending from polar plumes and streamers down to scales in the kilometer size range at the Sun, this study was undertaken to further characterize the fine-scale structures using the unique probing abilities of radio occultation measurements. Of particular interest were the differences between the structures in the fast wind emanating from coronal holes and those in the stalks of coronal streamers, the source of the slow wind.

While earlier studies established that the density variations across the filamentary structures arc an order of magnitude higher in the slow than fast solar wind, this paper demonstrates that the structures arc also finer by more than a factor of three in the slow than fast solar wind, Since the base of coronal streamers is dominated by closed loop-like magnetic structures, it seems plausible that the open field lines originating from these regions, and forming the stalks of the streamers, arc more sparsely distributed and more tightly constricted, in coronal holes, on the other hand, the predominance of open magnetic field structures allows a larger number to expand more readily, Consequently, one would expect the filamentary structures to be. finer in the slow solar wind associated with corona] streamers than the fast wind emanating from coronal holes.

The sizes of finest filamentary structures have been obtained by taking advantage of (1) our understanding of the relationship between flux tube size, high anisotropy of angular broadening, and break in the density spectrum, (2) gains in knowledge of the morphology of the corona, allowing the slow solar wind to bc distinguished from the fast wind, and (3) the availability of velocity estimates to support the slow wind and distinguish coronal streamer from propagating disturbance. The sizes of the finest structures could bc inferred from the density spectra only because the latter were determined with great precision, a testament to the fine measurements of phase scintillation and spectral broadening by the NASA Deep Space Network and the robustness of their interpretation.

The results of this paper were obtained from temporal (phase scintillation and spectral broadening) rather than spatial (angular scattering) measurements because the former have been more systematical] y investigated and reported. Still, size information from angular scattering measurements would bc preferred, because angular scattering measures spatial scales directly. Since a decrease in finest filamentary structure size is manifested as an increase in anisotropy, the results of this paper predict that the passage of a coronal streamer would appear as a 'transient' in angular scattering measurements, and that the enhancement in scattering would bc accompanied by a rise in anisotropy. While this

behavior may have been observed in individual and unpublished transients (private communication with W.C. Erickson and M.J. Mahoney), it is apparently manifested in the reported solar cycle dependence of angular scattering measurements. Anisotropy has been observed to be higher during solar maximum than solar minimum [Blessing and Dennison 1972, Ward 1975, Armstrong et al. 1990], implying that the finest filamentary structures are smaller during solar maximum, and consistent with the fact that white-light measurements show a corona more filled with streamers during solar maximum.

The near-Sun slow and fast wind spectra in Fig. 3 are similar to and closely related to spectra observed by in situ and scintillation measurements beyond 0.3 AU [Marsch and Tu 1990, Manoharan et al, 1994]. It is interesting that investigations of plasma properties based on in situ density measurements suggest flux tubes or spaghetti-like structures corresponding to fluctuation frequencies lower than 10^{-4} Hz [Tu et al. 1989; Thieme et al. 1989; Tu and Marsch 1990; Marsch and Tu 1994]. Still, without the benefit of imaging or spatial measurements such as those provided by angular broadening in the case of radio occultation measurements, one can never be sure about the identification of spatial structures in in situ plasma measurements. A systematic global study of the break in the density spectrum is currently being carried out based on extensive phase scintillation measurements over a wide range of heliocentric distances. Results from this investigation and comparisons with those from in situ measurements beyond 0.3 AU should lead to an improved understanding of the relationship between these two types of measurements (path-integrated and point), and the morphology and evolution of the finest raylike structures in the solar wind. The existence of different size flow tubes in the solar wind could have significant implications for our understanding of the processes defining the characteristic differences bet wccn the fast and slow solar wind,

We would like to thank J.W. Armstrong, B. Bavassano, W.C. Erickson and M.J Mahoney for useful discussions, P. Gazis for kindly computing the heliographic

coordinates of the closest approach points, and the referee whose comments improved the paper. The research carried out at the Jet Propulsion Laboratory, California Institute of Technology was supported by a contract with the National Aeronautics and Space Administration. Support for S. R. Habbal was provided by NASA grant NAGW-438 1 to the Smithsonian Astrophysical observatory.

REFERENCES

Anantharamaiah, K. R., Gothoskar, P., & Cornwell, T.J. 1994, J. Astrophys. Astr., 15, 38'7

Armstrong, J. W., Coles, W. A., Kojima, M., & Rickett, B.J.1990, ApJ., 358, 685

Blessing, R. G., & Dennison, P.A.1972, Astr. Sot. Aust., 2, 84

Callahan, P.S. 1975, ApJ.,199, 227

Colts, W.A. 1978, Space Sci. Rev., 21,411

Colts, W, A., Liu, W., Harmon, J. K., & Martin, C. I,. 1991, J. Geophys. Res., 96, 174S

Cronyn, W.M. 1970, ApJ., 161, 755

—. 1972, Ap. J., 171, L101

Erickson, W.C. 1964, ApJ., 139, 1290

Gosling, J.'J'., Borrini, G., Asbridge, J. R., Bame, S. J., Feldman, W. C., and Hansen, R. T'. 1981, J. Geophys.Res., 86, S438

Hewish, A. 1958, Mon. Not. Roy. Astr. Sot., 118, 534

Hewish, A. 1971, Ap. J., 163, 645

1 locksema, J.'l'., & Scherrer, P.J. 1986, WDC-A for Sol-l'err. Phys., Rept. UAG-94

Huddleston, D.E., R. Woo, & M. Neubebauer 1995, J. Geophys. Res., 100, 19951

Jokipii, J. Il. 1973, Ann. Rev. Astron. Astrophys., 11, 1

Karovska, M. & Habbal, S.R. 1991, Ap. J., 371, 402

Koutchmy, S. 1988, in Solar and Stellar Coronal Structure and Dynamics, cd. R. Altrock, NSO/S.P. Workshop, 208

Lotova, N.A. 1975, Sov. Phys.-Usp., 18, 292

Manoharan, P. K., Kojima, M., & Misawa, 11.1994, J, Geophys. Res., 99, 23411

Marsch, E., Tu, C.-Y. 1990, J. Geophys. Res., 95, 11945

Marsch, E., & Tu, C.-Y. 1994, Ann. Geophys., 12, 1127

Martin, J.M. 1985, PhD thesis, Stanford University, Stanford, CA

Narayan, R., Anantharamaiah, K. R., & Cornwell, T.J. 1989, Mon. Not. Roy. Astr. Sot., 241,403

November, L. J., & Koutchmy, S. 1996, ApJ, 466, 512

Thieme, K. M., Schwenn, R., & Marsch, E. 1989, Adv. Space Res., 9, 127

Tu, C.-Y, & Marsch, E. 1990, J. Geophys. Res., 95, 4337

Tu, C.-Y., Marsch, E., & Thieme, K.M. 1989, J. Geophys. Res., 94, 11739

Vitkevitch, V.V. 1959, in Paris Symposium on Radio Astronomy, cd. R.N. Bracewell, (Stanford: Stanford University Press), 275

Ward, 13.1>.1975, PhD thesis, University of Adelaide

Winterhalter, D., Smith, E. J., Burton, M. E., Murphy, N., & McComas, D. J., J, Geophys. Res., 99, 1994.

Woo, R. 1993, J. Geophys. Res., 98, 18999

· . 1995, Geophys. Res. Lett., 22, 1393

· · · 1996, Nature, 379, 321

Woo, R., & Armstrong, J.W. 1979, J. Geophys. Res., 84, 7288

-.1981, Nature, 292, 608

Woo, R., & Gazis, P. 1993, Nature, 366, 543

Woo, R., & Schwenn, R. 1991, J. Geophys. Res., 96, 21227

Woo, R., Yang, F.-C., Yip, K. Y., & Kendall, W.B. 1976a, ApJ., 210, 568

Woo, R., Yang, F.-C., & Ishimaru, A, 1976b, ApJ., 210, 593

Woo, R., Armstrong, J. W., Sheeley, Jr., N. R., Howard, R. A., Koomen, M. J., & Michels, D.J. 1985, J. Geophys. Res., 90, 154

Woo, R., Armstrong, J.W., Bird, M. K., & Pätzold, M. 1995, ApJ., 449,1.91

1.1ST OF FIGURES

Fig. 1 Schematic illustration of the observation of radially expanding flux tubes by the VI .A and Culgoora observatories, with interferometer baselines of 1-35 km and 0.2-2 km, respectively. The circles depict the longest baselines and hence the larges scales probed,

Fig. 2 Schematic log-log diagram of structure function near the Sun. Inside the flux tube (scale s smaller than the flux tube size D), the convected small-scale turbulence is nearly isotropic and the structure function parallel and transverse to the magnetic field B varies approximately as s^1. For distances exceeding the flux tube size D, it steepens to $s^{5/3}$ (Kolmogorov case) transverse to the magnetic field B, but continues to vary as s^1 parallel to B. The latter is dashed when s is large to stress the absence of relevant measurements.

Fig. 3 Reproduced from Fig. 3a of Colts et al. [1991] showing 11 structure functions over the heliocentric distance range of 7.1-9.8 R_0. The structure functions have been converted back to the originally measured density spectra by adding a frequency scale to the abscissa; note that frequency increases from right to left. The uppermost density spectrum is of the slow solar wind observed by Voyager 2 on August 17, 1979 (DOY 22.9), while the lowermost spectrum is of the fast wind observed by Voyager 2 on September 20, 1980. The arrows indicate the breaks in the density spectra occurring at 0.76 and 2.6 Hz for the slow (uppermost curve) and fast (lowermost curve) wind, respectively.

Fig. 4 Contour maps of source surface coronal magnetic field strength at 2.5 R_0 produced by the Wilcox Solar Observatory [Hocksema and Scherrer 1968] for (a) CR 1684 and (b) CR 1699. The closest approach point of August 17, 1979 (DOY 229) is projected onto the relevant map of CR 1684 (indicated by the dot) showing that a region of evolving heliospheric current sheet and consequently slow solar wind was probed. The closest projected approach point of September 20, 1980 (DOY 264) shows that it probed the fast wind emanating from a coronal hole during CR 1699.

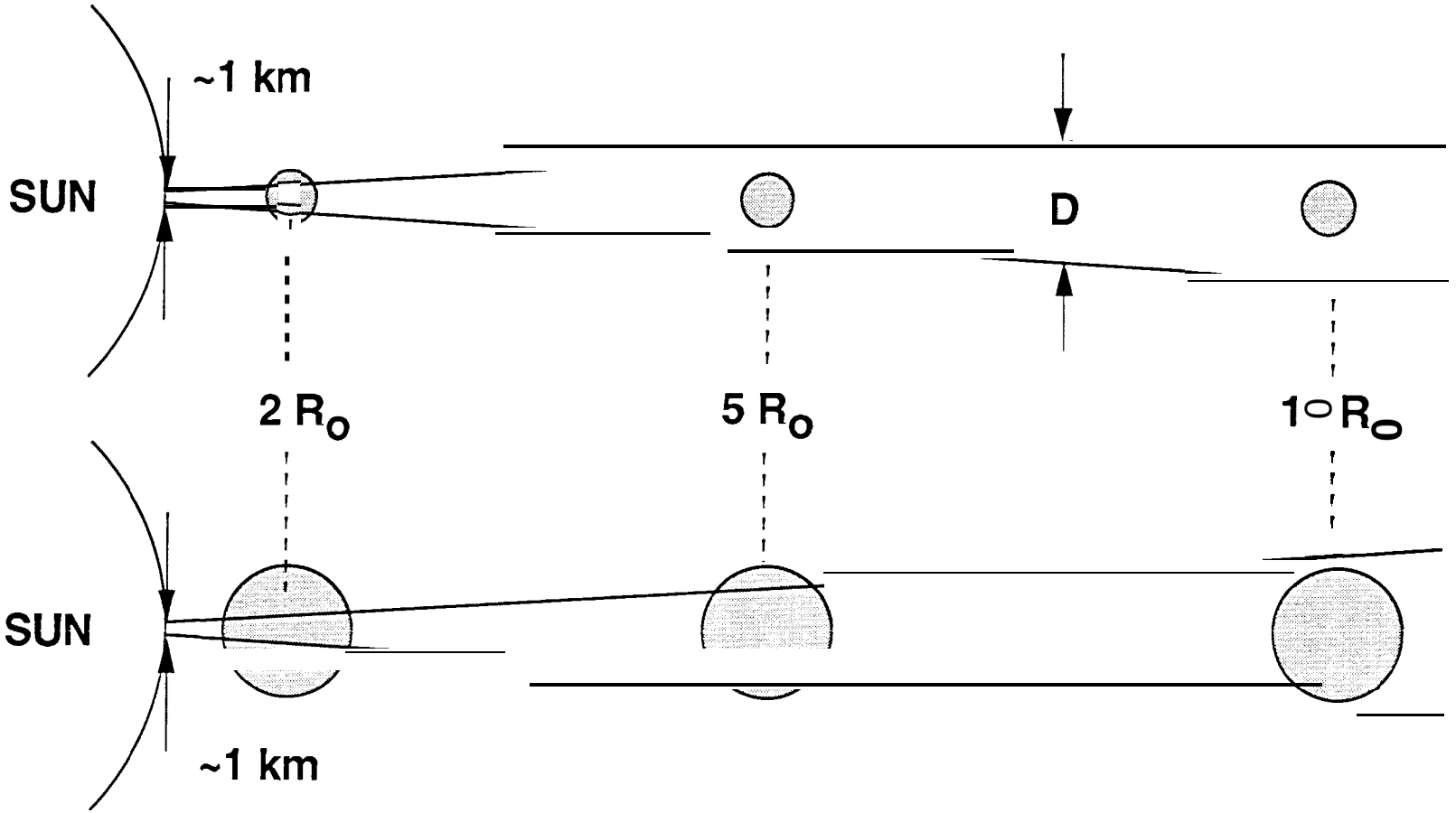
Culgoora (baselines 0.2-2 km)
~1 km
SUN
D
2 R_o
5 R_o
10 R_o
SUN
~1 km
VLA (baselines 1-35 km)

Fig.

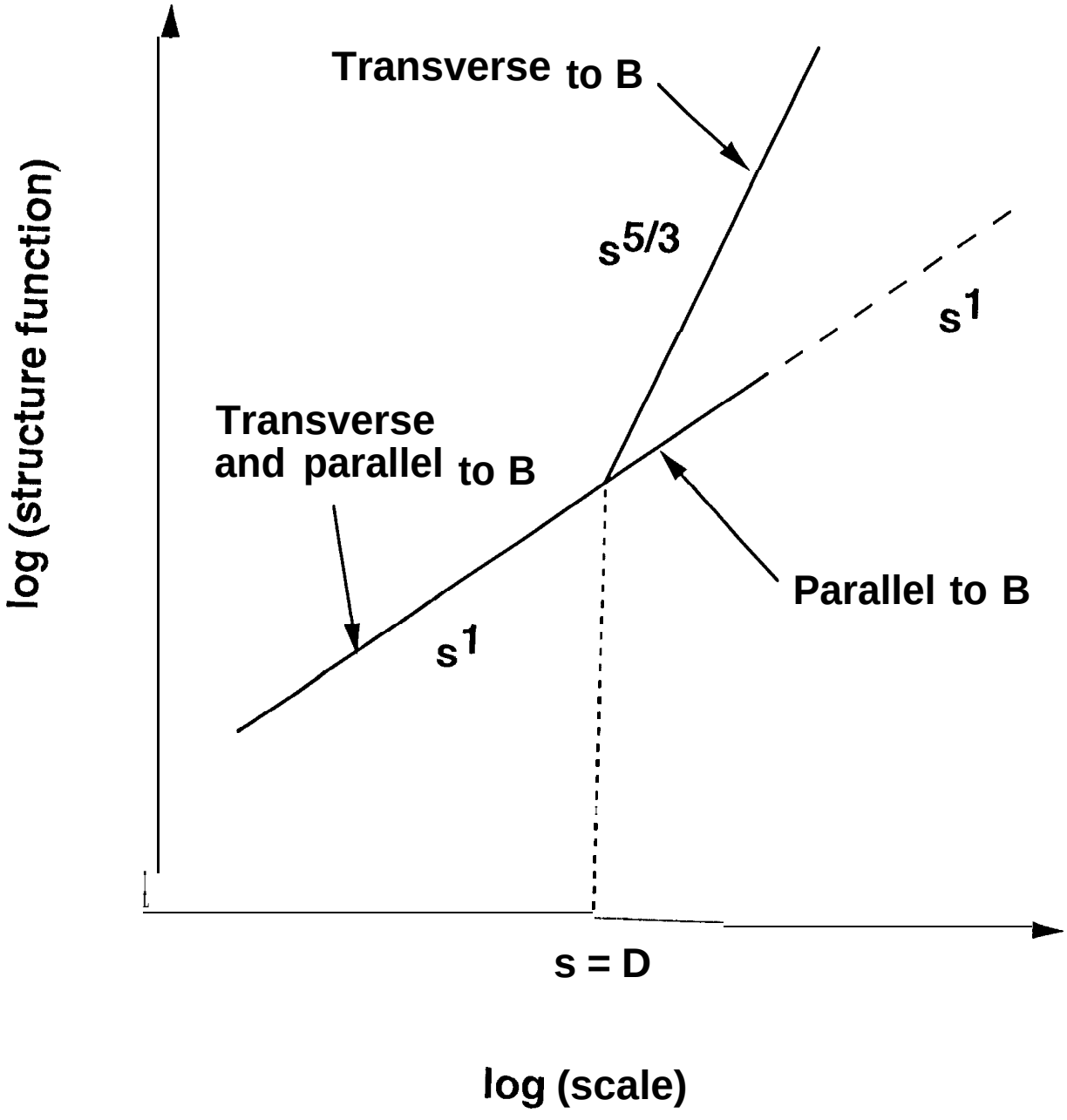
Transverse to B
$s^{5/3}$
s^1
Transverse and parallel to B
Parallel to B
s^1
log (structure function)
s = D
log (scale)

Fig. 2

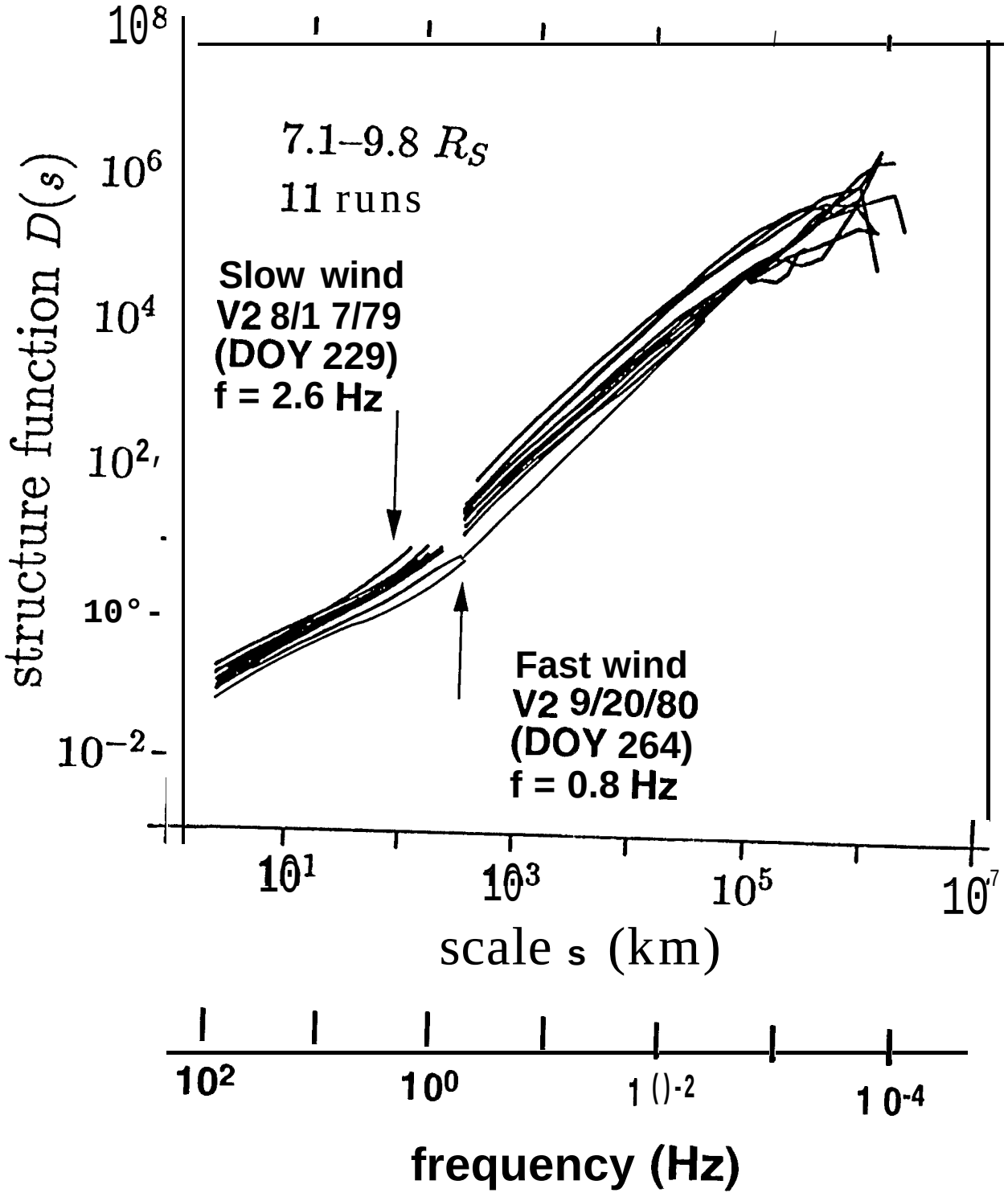
7.1–9.8 R_S
11 runs
Slow wind
V2 8/1 7/79
(DOY 229)
f = 2.6 Hz
Fast wind
V2 9/20/80
(DOY 264)
f = 0.8 Hz
structure function $D(s)$
10^8
10^6
10^4
10^2
10^0
10^{-2}
10^1
10^3
10^5
10^7
scale s (km)
10^2
10^0
10^{-2}
10^{-4}
frequency (Hz)

Fig. 3

(a)

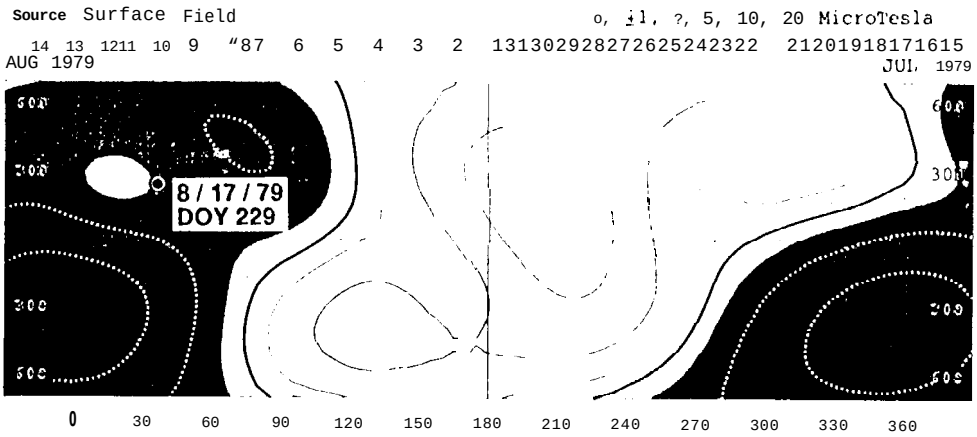

1684

(t))

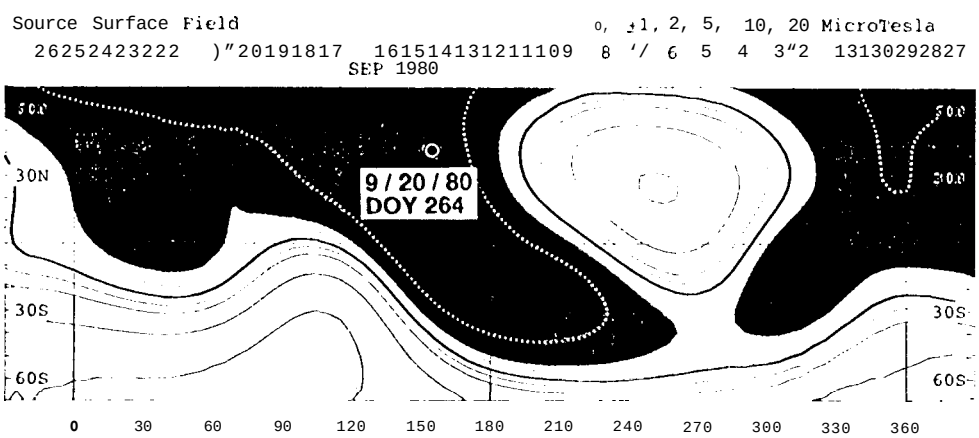

1699

Fig. 4